Single Crystalline Nanowires of Lead: Large-Scale Synthesis, Mechanistic Studies, and Transport Measurements†

Yuliang Wang,‡ Xuchuan Jiang,‡ Thurston Herricks,§ and Younan Xia*,‡

Department of Chemistry and Department of Materials Science and Engineering, University of Washington, Seattle, Washington 98195-1700

Received: September 15, 2003; In Final Form: November 13, 2003

A solution-phase, precursor method has been demonstrated for the large-scale synthesis of single crystalline nanowires of lead with uniform diameters in the range 50−90 nm and lengths up to several millimeters. In a typical procedure, the nanowires were synthesized by refluxing a mixture of $Pb(CH_3COO)_2 \cdot 3H_2O$ and poly(vinyl pyrrolidone) (PVP) in ethylene glycol under N_2 for 90 min. Elemental lead was generated as a result of thermal decomposition of the precursor salt. Electron microscopic studies indicated that a solution−liquid−solid (SLS) growth mechanism was responsible for the nucleation and growth of lead atoms into single crystalline nanowires. When the hot reaction solution was injected into a cold ethanol bath through a syringe needle, bundles made of uniaxially aligned lead nanowires were formed. It was found that both composition and morphology of the product had a strong dependence on the reaction conditions that included the molar ratio between PVP and lead acetate, the reaction temperature, and the environment (nitrogen versus air). As the parameters were varied, nanostructures with a range of morphologies and compositions were observed as the products. Transport measurements on individual lead nanowires (as thin as ∼50 nm in diameter) suggest a transition to the superconducting state around 7.13 K, a temperature similar to the value (7.20 K) reported for bulk lead.

Introduction

One-dimensional (1D) nanostructures (in the form of wires, rods, belts, and tubes) have received considerable attention in recent years due to their novel properties and intriguing applications in a number of different areas.[1] Metal nanowires, for example, have been the focus of many studies for their important roles as active components and/or interconnects in fabricating nanoscale electronic or optoelectronic devices.[2] Among various metals that have been studied as nanowires, lead is a particularly attractive, important, and challenging target as a result of its superconductivity and high reactivity.[3] Uniform nanowires of lead are usually synthesized via electrochemical deposition by templating against channels etched in various porous membranes or atomic steps on various solid substrates.[4] Although the use of physical templates may have the advantages of predefined 1D morphology and controllable wire diameters, there are also a number of intrinsic shortcomings or limitations: First of all, the total number of wires that can be produced in each run of synthesis is restricted by the density of channels in a membrane or the number of steps on a substrate. For a typical polycarbonate or anodic alumina membrane, the density of pores is usually below 10^{12} /cm^2. Second, it still remains a grand challenge to form nanowires longer than 20 μm by templating against porous membranes. Third, most of the samples prepared by using the template-directed method were polycrystalline, although it was possible (as demonstrated by Schwarzacher et al.[4c] and Jalochowski et al.[4d,4e]) to generate single crystalline lead nanowires by carefully controlling the conditions for electrochemical deposition. Fourth, any defects on the surface of the channels would result in the formation of nanowires with poorly defined structures and shapes, i.e., kinks or nonuniform thicknesses. The last but not least, additional steps are often required in order to separate the nanowires from the template and obtain individual nanowires for use in property measurements or device fabrication.

We have recently demonstrated a solution-phase approach that generated silver nanowires with uniform diameters and in large quantities by reducing silver nitrate with ethylene glycol in the presence of poly(vinyl pyrrolidone) (or PVP).[5] In this so-called "polyol process", which has been extensively exploited by other groups for the synthesis of metal nanoparticles, ethylene glycol serves as both reducing agent and solvent for the reaction. The key component of this synthesis is PVP that acts as a capping reagent to confine and direct the growth of seeds into 1D nanostructures. In the present study, the similar polyol method (but with a different mechanism) was employed to generate single crystalline nanowires of lead with long, uniform diameters and in copious quantities. More specifically, the production of lead nanoparticles, i.e., the initial step, was realized via the thermal decomposition (instead of reduction as it was for silver) of a lead precursor salt, $Pb(CH_3COO)_2 \cdot 3H_2O$, in boiling ethylene glycol under the protection of N_2. Here ethylene glycol merely served as a high-boiling-point solvent, which could be refluxed at a temperature sufficiently high to initiate and maintain the thermal decomposition of lead acetate. As refluxing was continued, small nanoparticles of lead were produced through homogeneous nucleation, and some of them further grew into micrometer-sized crystals. These microcrystals could serve as the roots in subsequent steps to initiate the growth of lead nanowires. The small lead nanoparticles remained in the solution would continuously provide a source of lead atoms

† Part of the special issue "Alvin L. Kwiram Festschrift".

* To whom correspondence should be addressed. E-mail: xia@chem.washington.edu.

‡ Department of Chemistry.

§ Department of Materials Science and Engineering.

10.1021/jp036758x CCC: $27.50
Published on Web 01/20/2004

for prolonged wire growth through processes such as Ostwald ripening. Experimental evidences also indicated that a solution−liquid−solid (SLS) growth mechanism was involved in the initiation and growth of single crystalline lead nanowires. In general, each nanowire was composed of three components: root (the microcrystal), stem (the nanowire), and tip (the liquid droplet of lead). After the solution had been refluxed under N_2 for 90 min, single crystalline nanowires of lead with diameters in the range 50−90 nm and lengths up to several millimeters could be easily separated from the hot reaction mixture by centrifugation. Compared to template-directed synthesis, our method allowed for the production of uniform lead nanowires in bulk quantities (i.e., on a scale close to the Avogadro's number). Different reaction conditions (e.g., the molar ratio between PVP and lead acetate, the temperature, and the reaction environment) were all found to have a profound impact on the morphologies and compositions of the final products. The electron transport properties of these lead nanowires were also studied in this work, and measurements on individual wires (with diameters down to ∼50 nm) suggest a transition to the superconducting state around 7.13 K.

Experimental Section

Chemicals and Materials. Anhydrous ethylene glycol (EG, 99.8%, Aldrich or Fisher), lead acetate trihydrate ($Pb(CH_3COO)_2 \cdot 3H_2O$, 99+%, Aldrich), poly(vinyl pyrrolidone) (PVP, $M_w \approx 55\,000$, Aldrich), and ethanol (200 proof, Aaper) were all used as received without further purification.

Synthesis of Lead Nanowires. Uniform nanowires of lead were generated by refluxing an ethylene glycol (Aldrich) solution that contained both lead acetate (the precursor) and PVP. In a typical synthesis, 0.1 g of $Pb(CH_3COO)_2 \cdot 3H_2O$ and 0.1 g of PVP were separately dissolved in 5 mL ethylene glycol and then simultaneously added dropwise (using pipets) into 10 mL of boiling ethylene glycol hosted in a three-neck flask. The reaction was protected with a continuous flow of N_2 gas and kept under constant magnetic stirring. A Glas-Col hemispherical heating mantle (Series O, 380 W, ChemGlass) was used to provide the heat required for this reaction. As the reaction proceeded, the solution underwent gradual changes in color from clear, colorless (0 min) to light yellowish opaque (∼25 min), then brownish gray (∼45 min), and finally dark black turbid (∼90 min). Darkening of the reaction mixture indicated the appearance of lead due to the thermal decomposition of the precursor salt and its continuous increase in quantities. After the reaction had been refluxed for about 90 min, the final product, i.e., lead nanowires, had to be collected by centrifuging the hot solution at 4000 rpm. In more detail, the hot reaction mixture was poured directly into a glass centrifugation tube within a few seconds and immediately centrifuged for 3 min. The supernatant was carefully decanted and ethanol was added to wash off the PVP and residual EG from the collected black precipitate (lead nanowires) in the tube. After another step of centrifugation, the cleaned nanowires were collected and stored in a desiccator under the protection of N_2 for future use. If necessary, the washing process could be repeated several more times until all the residual PVP and EG had been removed. It has been found that if the synthesis was carried out in EG that was purchased from Fisher, additional 30−60 min may be required in order to get complete reaction.

For electron microscopic studies, the samples were prepared as follows: a small portion of the reaction mixture (∼1 mL) was taken out of the flask during reaction using a pipet and then transferred into a microcentrifugation tube and centrifuged quickly in a microcentrifuge (Model V, VMR Scientific) at a speed of 10 000 rpm for 3 min. The collected sample was then washed with ethanol and the dispersed on a silicon substrate or TEM grid.

Formation of Bundles of Uniaxially Aligned Nanowires. After the reaction had proceeded for 90 min, the hot reaction mixture was drawn into a 10-mL glass syringe (MICRO-MATE interchangeable, Popper & Sons) through a stainless steel needle. Without delay, the solution was quickly injected into 500 mL of cold ethanol hosted in a 1000-mL beaker, which had been cooled in a freezer in advance. Precipitates with a threadlike morphology could be observed instantly after the injection. The supernatant was decanted carefully after all solids had settled down to the bottom of the beaker. In the following step, fresh ethanol was added slowly to the beaker to rinse the precipitates. After filtration through a membrane, the nanowire bundles were dried in a desiccator connected to an aspirator and stored in an inert environment.

Transport Measurements. In a typical procedure, a freshly prepared nanowire of lead was deposited from a very dilute dispersion in ethanol (via slow solvent evaporation) onto four gold electrodes (10 μm wide, 200 nm thick, and separated by 25 μm) that had been patterned on a glass substrate (micro slides 2947, Corning). Due to the low melting point of lead, a good contact between the lead nanowire and the gold electrode could be ensured via brief heating by focusing the electron beam of a scanning electron microscope on the contacted region. For the same reason, the currents used in all measurements were kept below 1.5 μA to avoid possible melting of the nanowires. Silver paste (Chemtronics, Kennesaw, GA) and copper wires were used to connect the pads of gold electrodes to the instrument. A Keithley 236 sourcemeter was used to supply the current and voltages were measured using a Keithley 155 microvoltimeter. A continuous flow cryostat (SuperTran-VP, Janis Research) was used to conduct the measurements of resistance at temperatures down to 4.2 K.

Instrumentation. Scanning electron microscopy (SEM) images were taken using a field emission microscope (Sirion, FEI, Portland, OR) operated at an acceleration voltage of 5 kV. Transmission electron microscopy (TEM) images and selected area electron diffraction (SAED) patterns were taken using a JELO-EX II microscope operated at 80 kV. The samples were prepared by placing one drop of the alcohol suspension on a silicon substrate or TEM grid and dried in a desiccator connected to an aspirator. High-resolution TEM (HRTEM) images were taken using a TOPCON 002B microscope operated at 160 kV. Powder X-ray diffraction (XRD) patterns were recorded from a large quantity of lead nanowires supported on a glass slide (micro slides 2947, Corning) using a Philips PW1710 diffractometer (Cu Kα radiation, $\lambda = 1.540\,56$ Å) at a scanning rate of 0.02° per second for 2θ in the range from 10° to 70°.

Results and Discussion

Microscopic Studies on the Formation of Lead Nanowires. To understand the reaction mechanism (such as the evolution in morphology and composition), samples were collected at different times and characterized by using both SEM and TEM. Figure 1 shows SEM and TEM images of samples collected at 20, 30, 45, and 60 min after lead acetate and PVP had been introduced, indicating all major distinctive morphologies associated with various stages of the reaction. Figure 1A shows an SEM image of the solid sampled at 20 min, where platelike whiskers with lengths around tens of micrometers and widths of several micrometers were the major product. Further XRD

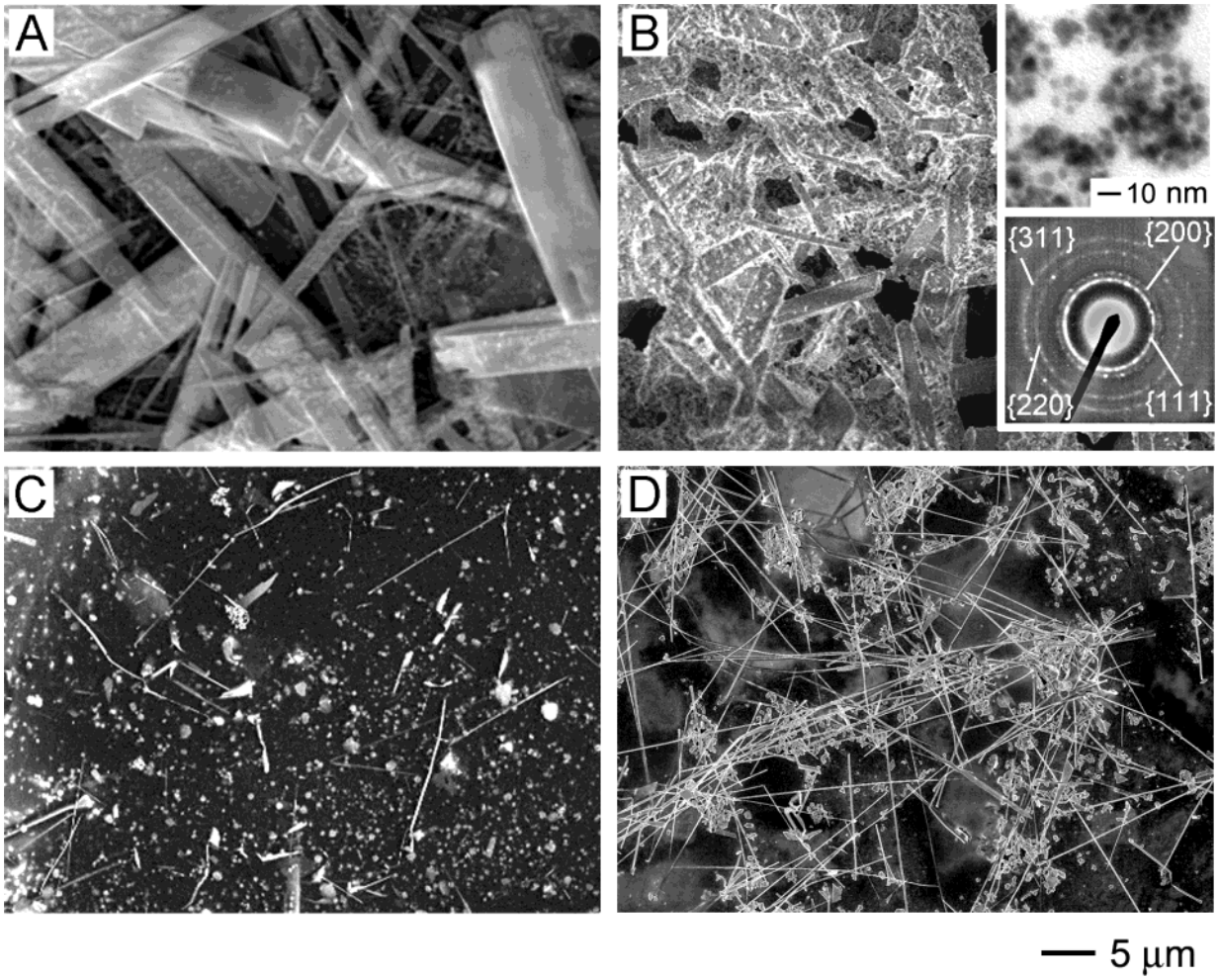

Figure 1. SEM images of four samples collected at different times after lead acetate had been introduced into the boiling ethylene glycol: (A) 20, (B) 30, (C) 45, and (D) 60 min. Each sample is characterized by distinctive morphologies and compositions: (A) platelike whiskers of basic lead acetate; (B) whiskers of basic lead acetate and small (5−10 nm in diameter) nanoparticles of lead formed as a result of thermal decomposition (the insets show a TEM image of the lead nanoparticles and their corresponding electron diffraction pattern); (C) a mixture of growing lead nanowires, microcrystals, and nanoparticles; and (D) long nanowires of lead mixed with a small amount of lead microcrystals.

examination indicated that the composition of these whiskers was basic lead acetate, an intermediate often involved in the early stages of thermal decomposition of $Pb(CH_3COO)_2 \cdot 3H_2O$. As a matter of fact, a similar morphology was also observed by Mohamed et al. in their studies on the thermal decomposition of lead acetate in the solid phase.[6a] Figure 1B shows an SEM image of the sample collected at 30 min, where the appearance of many newly formed small nanoparticles can be easily identified. A small amount of whiskers (similar to those shown in Figure 1A, but with much smaller dimensions) could still be found in this sample. Both TEM and diffraction studies (see the insets of Figure 1B) indicated that the sizes of these small particles were only a few nanometers across and they were purely made of lead. As a result, the light yellowish color observed for the reaction mixture can be attributed to the Mie scattering of such nanoparticles of lead.

In the past, thermal decomposition of lead acetate in the solid state has been studied by a number of groups.[6] Depending on the temperature (up to 450 °C) and environment (under N_2 or in air), both Pb and PbO had been identified as the final products, together with several types of basic lead acetate as the intermediates. According to these studies, the minimum temperature required for the production of metallic lead was around 325 °C. Here we found that lead could be formed as the predominate product (together with the formation of acetic acid as a byproduct) when the decomposition reaction was performed in a liquid phase such as in ethylene glycol (bp =198 °C) and under the protection of N_2 gas. It is believed that the minimum temperature required to decompose lead acetate into metallic lead could be greatly reduced in the polyol process, as it was now dissolved in a solution in the form of molecular species. In addition, as discussed by Buhro et al. in their SLS growth of semiconducting nanowires,[7a] the use of a heating mantle (whose temperature could reach as high as 450 °C) might generate local hot spots on the wall of reaction container with their temperatures much higher than the boiling point of ethylene glycol. The thermal decomposition of lead acetate could thus be greatly facilitated due to the presence of such hot spots.

A control experiment was also carried out to verify that there was, in fact, no reduction function associated with ethylene glycol in the present synthesis. In this experiment, lead nitrite that has a much higher decomposition temperature (~470 °C) was added (together with PVP) to ethylene glycol and refluxed in the same way as we did for the thermal decomposition of lead acetate. No production of lead was observed, even after prolonged periods of heating to 5 h. This result suggested that the production of lead was not due to the reduction of Pb^{2+} by ethylene glycol but rather was due to thermal decomposition. In comparison with lead nitrate, lead acetate happened to decompose at a sufficiently low temperature to be used with ethylene glycol. For the sample collected at 45 min, the solution exhibited a brownish gray color, and an SEM image of this

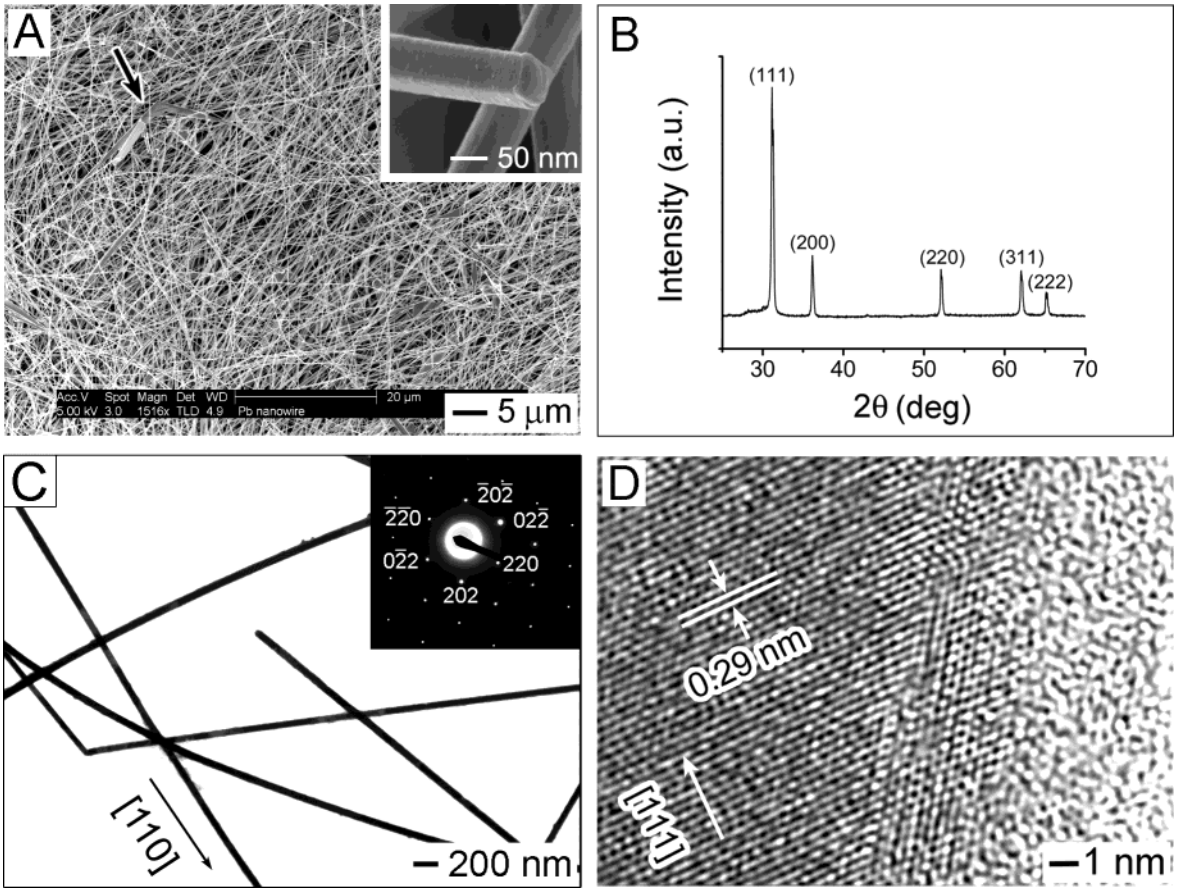

Figure 2. (A) Typical SEM image of the as-synthesized lead nanowires that were 85 ± 5 nm in diameter and up to several millimeters in length. The inset shows the cross section of a fractured nanowire. (B) XRD pattern recorded from the same batch of lead nanowires. (C) A TEM image of nanowires taken from the same sample as shown in (A). The inset gives a microdiffraction pattern recorded by focusing the electron beam on an individual wire. (D) HRTEM image taken from the edge of a lead nanowire. The fringe spacing along the [111] axis is indicated.

sample is given in Figure 1C. Compared to Figure 1B, no whiskers of basic lead acetate existed anymore, suggesting that all of them (produced in earlier stages) had been fully decomposed into elemental lead. In addition to small lead nanoparticles (similar to those appearing in Figure 1B), two new types of morphologies were found predominantly in this image: wirelike nanostructures of lead that represents the synthetic target of this work and micrometer-sized crystals that were also made of pure lead. For samples collected after the solution had been refluxed for 60 min, a typical SEM image is given in Figure 1D. Here we see mostly lead nanowires with lengths of up to tens of micrometers, together with a small portion of micrometer-sized crystals that were also observed for the sample collected at 45 min. However, only a small amount of lead nanoparticles (as those shown in Figure 1B) could be found in this sample. As the reaction time was further increased, the percentage of lead nanowires in the final product and the lengths of these nanowires were both greatly increased. For samples collected after the precursor salt had been introduced for 90 min, the yield of lead nanowires could approach 100%, with their lateral dimensions being uniformly distributed in the range 50−90 nm and lengths up to several millimeters.

Structural Characterization of the Lead Nanowires. After lead acetate had been refluxed with PVP in ethylene glycol for 90 min, the lead nanowires had to be harvested immediately through centrifugation (at 4000 rpm) while the reaction mixture was still hot. The collected solid was also washed with ethanol to remove excess PVP and EG coated on the nanowires. The as-obtained nanowires were often thinner than 90 nm in diameter and with lengths up to several millimeters. Studies by SEM and TEM (Figure S1) further indicated that about 80% of them had their diameters confined to the range of 75 ± 10 nm, albeit wires as thin as 30 nm could also be found in the final product. Figure 2A shows the SEM image of a typical sample (after PVP and EG had been removed), illustrating the uniformity, straightness along the long axis, and the copiousness in quantity that could be routinely achieved using this new synthetic approach. As indicated by an arrow, there was also a small amount of platelike structures in this sample, and the lead nanowires seemed to grow out of their tapered corners. These plates, in fact, had the same pure composition (Pb) as the particulate products shown in Figure 1C,D. The only difference was that each platelike crystal had at least one nanowire growing out of its tapered corners. As discussed in more detail later, these micrometer-sized plates actually served as the roots for the growth of long, uniform lead nanowires during the reaction. The inset of this image provides a closer look at the end of a fractured nanowire, and it clearly indicates that each lead nanowire synthesized using the present method had a rectangular cross section. Figure 2B shows the XRD pattern taken from the same batch of sample (in a bulk quantity), implying that the nanowires obtained using this solution-phase method crystallized purely in the face-centered cubic phase of lead.

Figure 2C shows a TEM image of several lead nanowires that were prepared from the same batch of sample shown in Figure 2A, and the uniformity in diameter along each individual wire could also be seen from this image. The inset displays a typical microdiffraction pattern that was obtained from an individual nanowire when the beam was oriented parallel to the [$\bar{1}$11] axis. All the diffraction spots could be indexed to the

face-centered cubic phase of lead. The diffraction pattern was essentially unchanged as the electron beam was scanned across each individual wire, suggesting that these lead nanowires were single crystalline in structure. Electron diffraction studies also indicated a growth direction along the [110] axis. The HRTEM image shown in Figure 2D was taken from the edge of a nanowire. With the use of fast Fourier-transfer technique, the lattice spacing of this single crystalline nanowire could also be resolved and indexed to that of face-centered cubic lead. Because the melting point of lead is relatively low (328 °C), the nanowire was highly susceptible to beam damage (especially for the relatively thinner region like the edge of a wire) when it was exposed to a flux of high-energy electrons. As a result, it is not unusual to observe that the right edge of this wire appears to have stacking defects, an artifact that might be caused by electron-beam-induced damage.

Mechanism for the Growth of Lead Nanowires. The growth of lead nanowires included at least four distinctive steps: (i) formation of elemental lead via the thermal decomposition of lead acetate, (ii) growth of the lead atoms into nanoscale particles through a homogeneous nucleation process, (iii) further growth of some lead nanoparticles into larger crystals (or roots) with their sizes on the scale of several micrometers, and (iv) nucleation and growth of nanowires from the corners of microcrystals at the expense of small nanoparticles as driven by Ostwald ripening.[8] This mechanism is consistent with all the images shown in Figure 1. With the sample collected at 45 min as an example, lead particles of two different sizes (micrometer versus nanometer) could be clearly seen in Figure 1C. This mechanism also resembles the one involved in the synthesis of silver nanowires, where silver particles of two distinctive sizes were found to coexist in the early stage of the reaction. It was further demonstrated that the silver particles of larger sizes could serve as seeds to initiate the growth of nanowires, as silver particles of smaller sizes were continuously dissolved into the solution phase and regrew onto the surfaces of larger ones as a result of Ostwald ripening. The growth should, in principle, continue until all the small particles had been completely consumed. However, there were some major differences between these two systems: (i) the roots of lead were single crystals with dimensions on the scale of micrometers while the seeds of silver were multiple-twined particles (MTPs) of only 20 to 30 nm in size; (ii) each lead nanowire was a single crystal with a rectangular-shaped cross section while the silver nanowire was multiply twined with a pentagonal cross section. On the basis of these observations, the growth mechanisms involved in these two systems should be different.

As we have noted in Figure 2A, the lead nanowire was often initiated from one of the corners of a micrometer-sized, platelike crystal. To better understand the growth mechanism, we carefully examined the sample collected at 60 min (the same as shown in Figure 1D) by electron microscopy and diffraction. Figure 3A−C shows the SEM images of several typical examples, illustrating how the nanowires were initiated and grew from the corners of roots. Despite their differences in sizes and shapes for the micrometer-sized crystals, all of them could serve as roots for the initiation of nanowire growth. Figure 3D shows the SEM image of a nanowire that had been fractured (by sonication) at a position close to the root. It is clear that this nanowire also exhibits a rectangular cross section similar to the one illustrated in the inset of Figure 2A. For the nanowire indicated by an arrow in Figure 3E, a spherical particle was also observed at the end opposite to the root. The inset of this image gives a blow-up view of the tip. Similar tip structures are also shown in Figure 3F,G, where two additional TEM images are given. Figure 3G, in particular, shows the TEM image of a wire that was still in its early stage of growth and both root and tip could be clearly observed in the same image. The presence of a root, and especially a particulate tip, on the opposite ends of a growing wire suggests that the growth of lead nanowires could share a mechanism similar to the solution−liquid−solid (SLS) process that has been explored by Buhro et al. and Korgel et al. for the synthesis of highly crystalline nanowires of various semiconductors.[7] A typical and important component of their synthesis was the use of a low melting point metal that could exist in the form of liquid droplets during the reaction. These liquid droplets could act as the solvent to dissolve (or suck in) the desired material in the form of atomic (or ionic) species. In the subsequent step, recrystallization could lead to the formation of nanowires or filaments with diameters of 10−150 nm and lengths up to several micrometers. In the present synthesis, most of the small lead nanoparticles produced via the thermal decomposition should be in their molten states because of the relative low melting point of lead. For particles that were able to grow into larger crystals through a homogeneous nucleation process, they should exist in the solid phase due to their enlarged dimensions (on the scale of micrometers). These large crystals could function as roots to initiate the growth of nanowires. As shown in Figure 3A−G, the wire growth normally started from the sharpest corner or thinnest end of a micrometer-sized root. For these regions with small areas and large curvatures, the surface atoms tended to be highly mobile and reactive at the boiling point of EG. As a result, lead atoms from the melted nanoparticles could be attracted to these reactive sites and eventually formed liquid droplets. Once the sizes of these liquid droplets had reached a critical value, the lead atoms would start to crystallize into a solid at the interface between the droplet and the root. As more lead atoms were driven into the droplets via Ostwald ripening, the growth could continue until all of the small lead nanoparticles had been completely consumed. Figure 3H shows a schematic illustration of this growth mechanism, where the root, stem, and tip of a nanowire are all specified.

We have also noticed that a large number of the lead roots displayed a planar or platelike morphology, and the wires growing out of the thin ends of these plates seemed to be coplanar with their roots. This is supported by the SEM image at the bottom of Figure 3I, which gives the side view of a nanowire that was still at its early stage of growth. The SAED patterns acquired from the root and stem regions of another nanowire are also shown as the insets of Figure 3I. Both of them exhibited the same type of diffraction spots with a hexagonal symmetry that are normally obtained when the beam direction is parallel to the [111] axes. Since the root of this nanowire had a platelike morphology, the placement of this plate should be parallel to the surface of the TEM grid. It is thus reasonable to conclude that both top and bottom surfaces of the thin plate were terminated in the {111} planes and that the wire growing out of the end of this plate was enclosed by the same set of planes. If we take a closer look at the pattern obtained from the root, it also exhibited some features that were not presented in the pattern taken from the stem. One feature is the appearance of diffraction rings that are usually associated with a polycrystalline material. Analysis on the *d* values of these rings indicated that they all originated from the face-centered cubic lead, similar to the index shown in Figure 1B. The appearance of these rings could be due to the deposition of some small lead nanoparticles onto the relatively large surfaces of

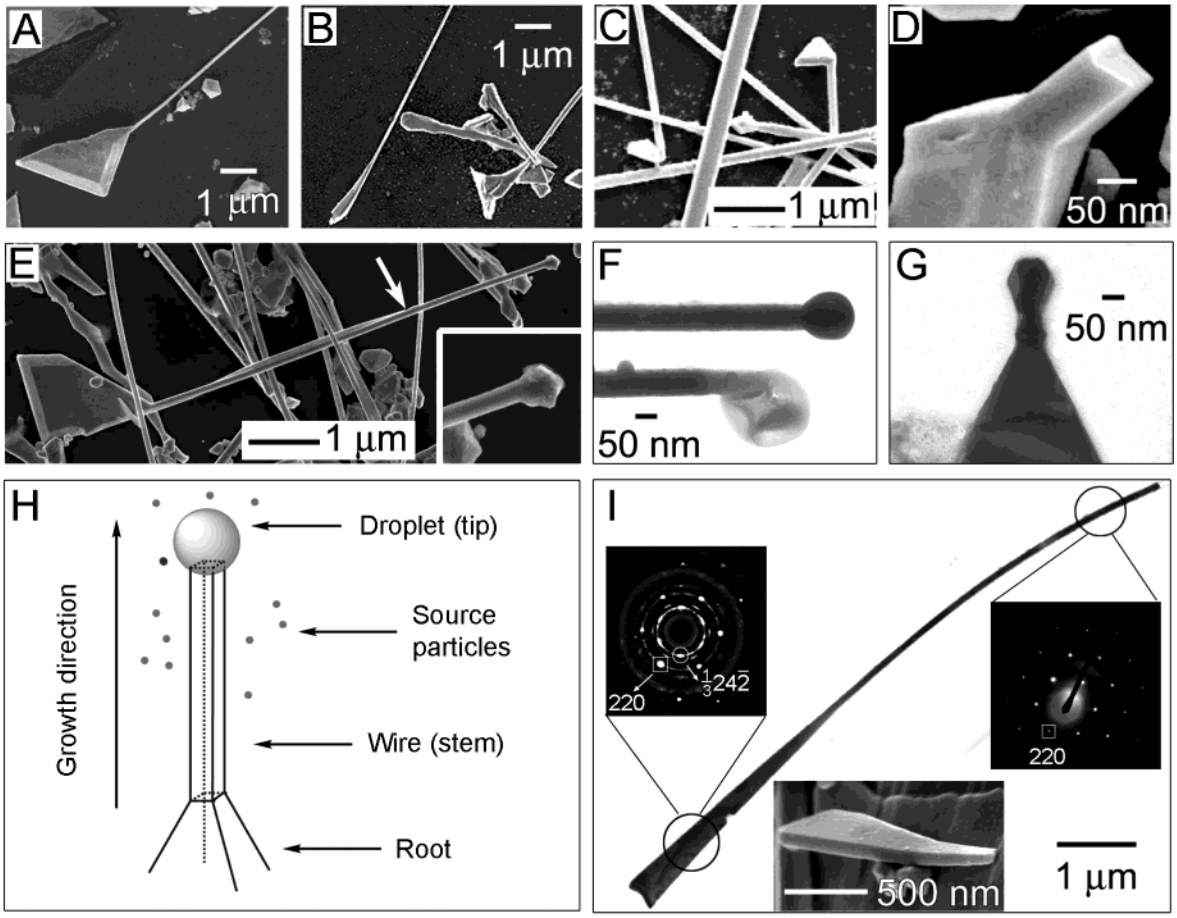

Figure 3. (A−D) SEM images of several lead nanowires, with focus on their roots. (E) The SEM image of a growing lead nanowire, showing both root and tip. The inset gives a magnified view of the tip. (F) A TEM image of two nanowires whose tips are terminated in droplets. (G) TEM image of another growing nanowire that was still at its early stage of growth, with its root, stem (wire), and tip all clearly recognizable. (H) Schematic illustration of the proposed mechanism responsible for nanowire growth. (I) TEM image of a growing nanowire and the SAED patterns (insets) recorded from its root and stem (wire), respectively. The side view SEM image of another wire at its early stage of growth, indicating that both root and stem of this wire were confined to the same plane.

the platelike root during sample preparation. Another feature is that there was also another set of diffraction spots with hexagonal symmetry located in the inner area of the diffraction pattern (as marked by a circle). These spots could be attributed to the (1/3){422} reflection that is forbidden for a face-centered cubic lattice. Because of the close match of their *d* values (2.90 Å versus 3.03 Å), these six spots overlapped with the {111} diffraction ring that originated from the small lead nanoparticles. As has been discussed in previous work on silver or gold nanostructures,[9] the apperance of these forbidden spots was often associated with thin structures that were enclosed by atomically flat top and bottom facets. It thus provides another piece of evidence to support our claim that the root is characterized by a platelike morphology, with a pair of flat {111} surfaces oriented parallel to the TEM grid.

Influence of the Molar Ratio between PVP and Lead Acetate. The exact role of PVP in controlling the formation of lead nanowires is yet to be completely understood. As established in a recent study related to the growth of silver nanowire,[5d] the PVP molecules were able to modulate the growth kinetics of a face-centered cubic metal by interacting with various crystallographic facets at different strengths. For example, the PVP molecules were found to interact more strongly with the {100} facets than with the {111} ones. This selectivity can be attributed to the difference in configuration for the atoms on these surfaces, which may enhance or hinder their coordination to the repeating units of PVP macromolecules. As a result, the side surfaces of a silver nanowire, enclosed by {100} planes, could be preferentially stabilized; while the ends, terminated in {111} planes, could be kept active for continuous growth. However, the PVP seems to play a different role in the synthesis of lead nanowires. As discussed above, the formation of highly anisotropic nanostructures was mainly directed by the liquid droplet at the tip of each growing nanowire. In this case, the kinetic effect (as mediated by the adsorption of PVP) seems to only play a minor role in inducing and maintaining 1D growth. We believe that the major function of PVP was to prevent the lead nanoparticles (which might also exist as liquid droplets in the boiling EG) from aggregating into large entities in the nucleation stage. As a result, only a small portion of the lead nanoparticles could grow into micrometer-sized crystals (or roots) and most of them were left in the solution to serve as a source for lead atoms in the growth step.

The percentage of lead nanowires in the final product, as well as the morphology of other lead structures produced during the reaction, was found to strongly depend on the molar ratio between PVP and lead acetate. When the ratio was around 3.5, the content of lead nanowires contained in the as-synthesized sample could approach 100%, as demonstrated by Figure 2A. However, if the ratio was decreased or increased to other values, lead structures of different morphologies were also found in the final product, with typical examples including belts and hexagonal (or triangular) thin plates. Depending on the exact value of this ratio, these new types of morphologies could even

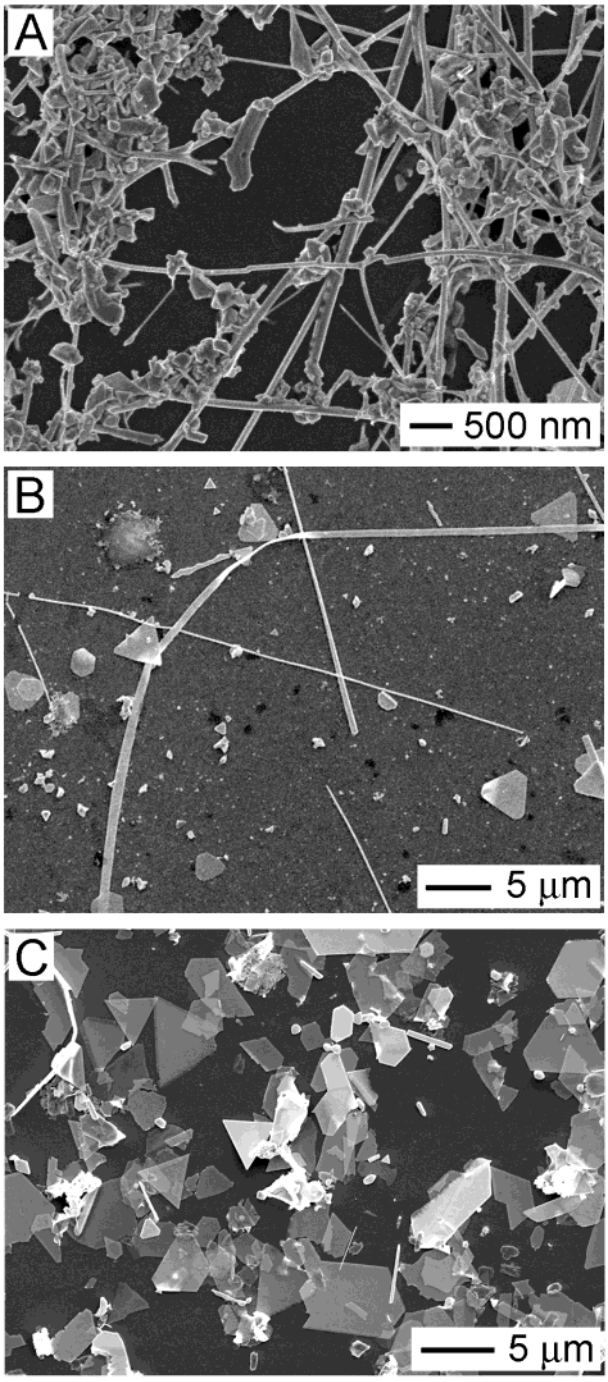

Figure 4. SEM images of three as-obtained samples illustrating the variation in morphology when nonoptimized molar ratios between PVP and $Pb(CH_3COO)_2$ were used: (A) 0; (B) 9; (C) 18. These structures were all made of pure lead, as confirmed by electron diffraction studies.

be obtained as the predominant ones in the final product. In these cases, lead nanowires only existed in relatively low quantities. Figure 4 shows the SEM images of three other samples that were prepared under a condition similar to the one used for Figure 2A, except that the molar ratio between PVP and lead acetate was varied to values other than 3.5. Figure 4A shows a typical image of the product where no PVP was added to the reaction mixture. This image implies that the same type of nanostructures as those shown in Figure 2A was formed, and some of them even showed the same root and stem structures when examined closely. The percentage of such wirelike structures were, however, much lower. The majority of structures in this sample exhibited irregular morphology and their sizes were normally on the micrometer-sized scales. This result suggests that, without the protection of PVP, most of the nanoparticles produced in the early stage preferred to grow into micrometer-sized roots, and only a small portion of the lead nanoparticles, which were still dispersed in the solution, could provide a very limited source of lead necessary for the continuous growth of leas nanowires. When this ratio was increased from 3.5 to 9 and 18, the final products were found to exist as sheetlike structures (Figure 4B) and hexagonal (or triangular) flakes (Figure 4C), respectively. Electron diffraction patterns taken from these structures indicate that they were all made of pure lead, with the flat surfaces being {111} planes. The appearance of these sheetlike structures might reflect the difference in interaction between PVP and various crystallographic planes, as we discussed for the preparation of silver nanostructures. A systematic study on this matter is under way.

Influence of the Reaction Temperature. Temperature was found to be another key factor that could affect the composition and morphology of the resultant product. Ethylene glycol had to be heated to its boiling point (i.e., ~198 °C) in order to initiate and maintain the decomposition of lead acetate into elemental lead. At temperatures lower than this value (e.g., at 190 °C), no elemental lead could be produced in the EG solution. Instead, several other types of lead salts (e.g., basic lead acetate and lead glycolate) were obtained as the final product, depending on the reaction time and temperature (in the range of 160 to 190 °C).

It was found that variation in temperature might also change the direction of reaction in the present synthesis. For example, after the reaction had proceeded for about 90 min and nanowires of lead had been produced in the form of a dark black, turbid solution, the reaction mixture could quickly fade into a clear light-yellow color within less than 10 min if heating was turned off. If this light yellow solution was heated to boil again, its dark color would be restored, and lead nanowires (of the quality and quantity similar to the sample shown in Figure 2A) could be obtained as the final product. We believed that the cause of this phenomenon was a result of the balance between two possible directions of a reversible reaction. When the temperature was sufficiently high, it could provide the heat required for the thermal decomposition of lead acetate, and elemental lead could be obtained as the predominant product, together with acetic acid as a major byproduct. If the temperature was lowered, the reaction direction would be reversed, and the lead nanowires would react with the acetic acid to produce lead acetate as the product. As shown by Sankarapapavinasam et al. in their studies on the corrosion rate of Pb in acetic acid,[10] at a relatively high temperature (e.g., immediately after heating was turned off), this reverse reaction was much faster when compared to the case at room temperature. As a result, the color of reaction solution quickly faded into light yellow. Since lead acetate can be easily dissolved in ethylene glycol, the resultant reaction mixture appeared as a clear solution. Figure 5 shows TEM images of a sample prepared from the light yellow solution, indicating the existence of very small nanoparticles with sizes around several nanometers. Electron diffraction pattern (the inset) taken from an assembly of these particles indicated that they were purely made of face-centered cubic lead. The light yellow color exhibited by the reaction solution could be attributed to the Mie scattering of the small lead nanoparticles stabilized by PVP macromolecules (same as for the sample obtained at the early stage of this synthesis). Since some of the acetate acid produced via thermal decomposition of lead acetate had been evaporated from the reaction mixture during the

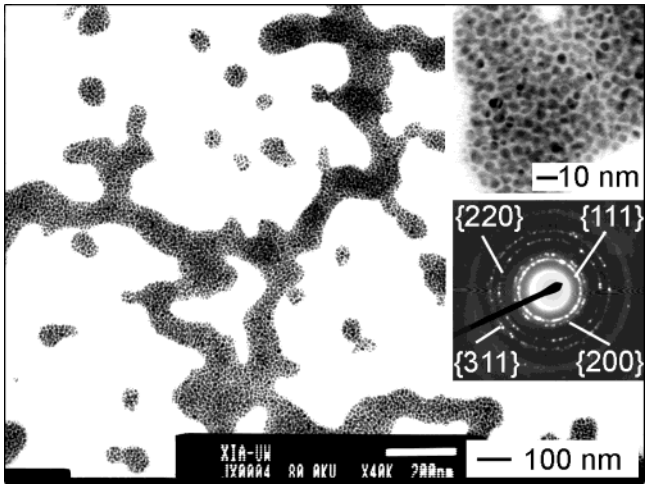

Figure 5. Influence of temperature on the morphology of resultant Pb nanostructures. The TEM image was taken from a sample prepared after the reaction solution had been cooled to room temperature. The insets give an enlarged view of the small nanoparticles and their corresponding SAED pattern.

refluxing process, elemental lead should be in excess when compared with the amount of acetic acid. As a result, a certain amount of the lead nanoparticles remained in the solution even after the reverse reaction had been completed. As limited by the reverse reaction, the separation of lead nanowires from the reaction mixture had to be completed within a couple of minutes while the solution was still hot.

Stability of the Lead Nanowires under Ambient Conditions. The lead nanowires had to be synthesized under the protection of an inert gas such as nitrogen or argon. Otherwise, elemental lead resulting from the thermal decomposition would be quickly oxidized at elevated temperatures (in particular, in the presence of CO_2 and O_2). After the nanowires had been separated from the reaction solution, it was also necessary to store them under an inert gas environment to prevent their surfaces from oxidation. As shown by Schwarzacher et al. in their TEM studies,[4d] a thin layer of PbO_2 would be readily formed on the surface of a lead nanowire after it had been exposed to air for a certain period of time. Here we also found that the lead nanowires tended to slowly change their morphology by reacting with gaseous species in the environment. Basic lead carbonate was identified as the major product by XRD studies, no matter if the lead nanowires were stored as a dry sample or as a suspension in ethanol. Figure 6A shows the SEM image of a dry sample after the lead nanowires had been exposed to the ambient environment of a chemical laboratory for 5 days. This image clearly indicates that the majority of lead nanowires had been converted to micrometer-sized flakes, whose appearance could be well-resolved in the inset. Figure 6B gives a typical XRD pattern recorded from this sample, indicating the coexistence of both elemental lead and basic lead salt, $Pb_3(CO_3)_2(OH)_2$. It was clear that the newly formed flakes shown in Figure 6A corresponded to the basic lead salt, which is a documented product for the reaction between Pb and H_2O under ambient conditions (i.e., in the presence of both O_2 and CO_2 gases).

Formation of Bundles of Uniaxially Aligned Lead Nanowires. The collection of lead nanowires from the hot reaction mixture was normally performed by centrifugation and then washed with ethanol to remove physically adsorbed PVP. As mentioned earlier, the collection process had to be performed quickly to avoid any possible reverse reaction between lead and acetic acid (another product of the thermal decomposition

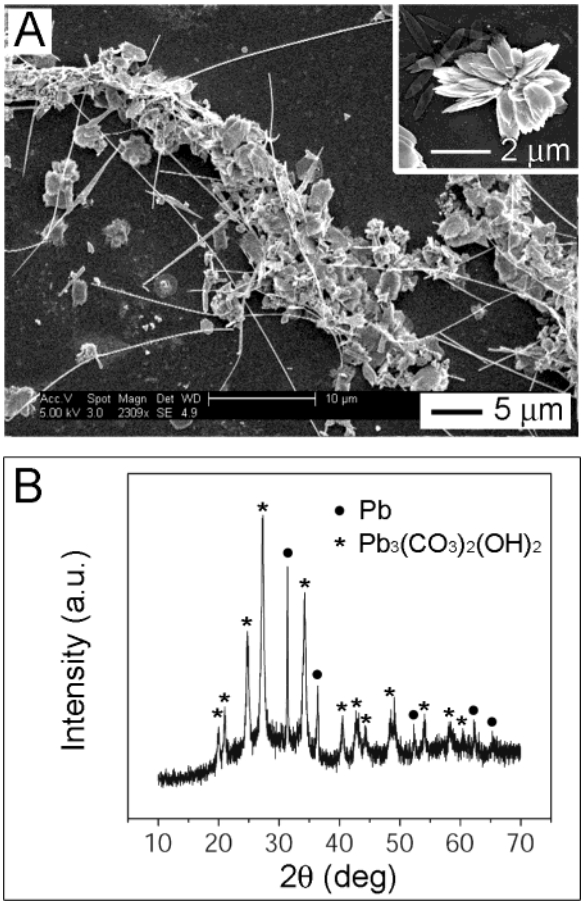

Figure 6. (A) SEM image of the same lead nanowires shown in Figure 2A, after the sample had been left in air for several days. The inset gives a closer look at the newly formed flakes of basic lead carbonate. (B) XRD pattern obtained from this sample, indicating the coexistence of both lead nanowires (dots) and basic lead carbonate particles (stars).

reaction). An alternative way to gather lead nanowires from the hot EG solution was to quickly quench the reaction solution by pouring the boiling mixture into a large quantity of cold ethanol. Here the ethanol played a role to abruptly reduce the temperature of the reaction system and to dilute the acetic acid to such an extent that the reverse reaction rate can be minimized. The solid that precipitated out in this process could then be collected using conventional centrifugation. We occasionally observed that the precipitate quenched out in the ethanol existed in a threadlike morphology, which could be as long as ~1 cm and even visible to the naked eye. A closer examination by SEM indicated that these threads were, in fact, thick bundles of many nanowires that were uniaxially aligned along other longitudinal axes. If we used a syringe to siphon the hot solution and immediately injected it into cold ethanol through a needle, most of the precipitates quenched out would exist in the threadlike morphology. They all contained bundles of uniaxially aligned nanowires when examined under an electron microscope. Figure 7 shows the low-magnification (Figure 7A) and high-magnification (Figure 7B) SEM images of a typical sample. From these two images, we can also readily appreciate the copiousness in quantity, uniformity in size, and relatively long length associated with the nanowires contained in the bundles, as well as the uniaxial alignment for nanowires within each bundle.

Electron Transport Properties of Individual Lead Nanowires. We note that several other groups have already observed the transition from metal to superconductor for lead nanowires prepared by templating against channels in porous membranes.[4a−c] All of their measurements were, however, performed on arrays

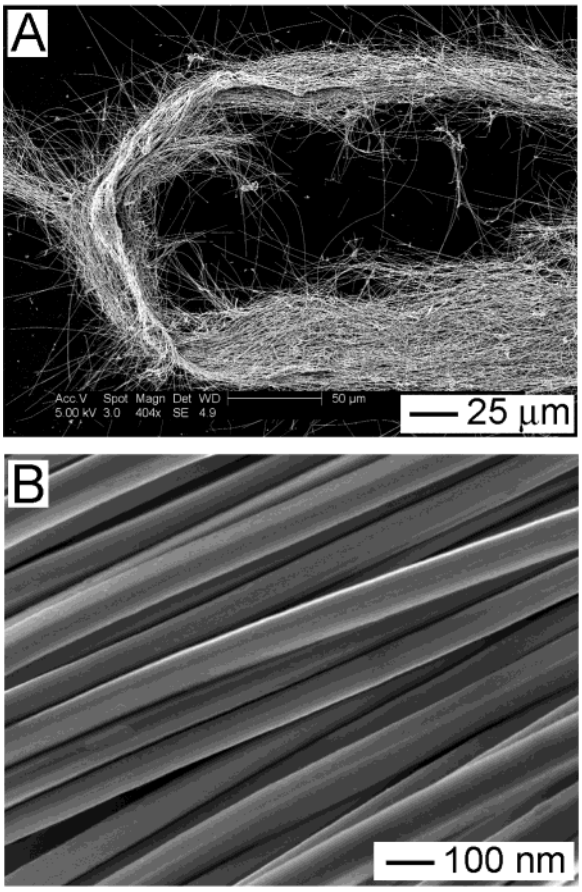

Figure 7. (A) Low-magnification and (B) high-magnification SEM images of a bundle of lead nanowires that was formed by injecting the wire dispersion into cold ethanol through a syringe needle. Note that the nanowires were uniaxially aligned within the bundle.

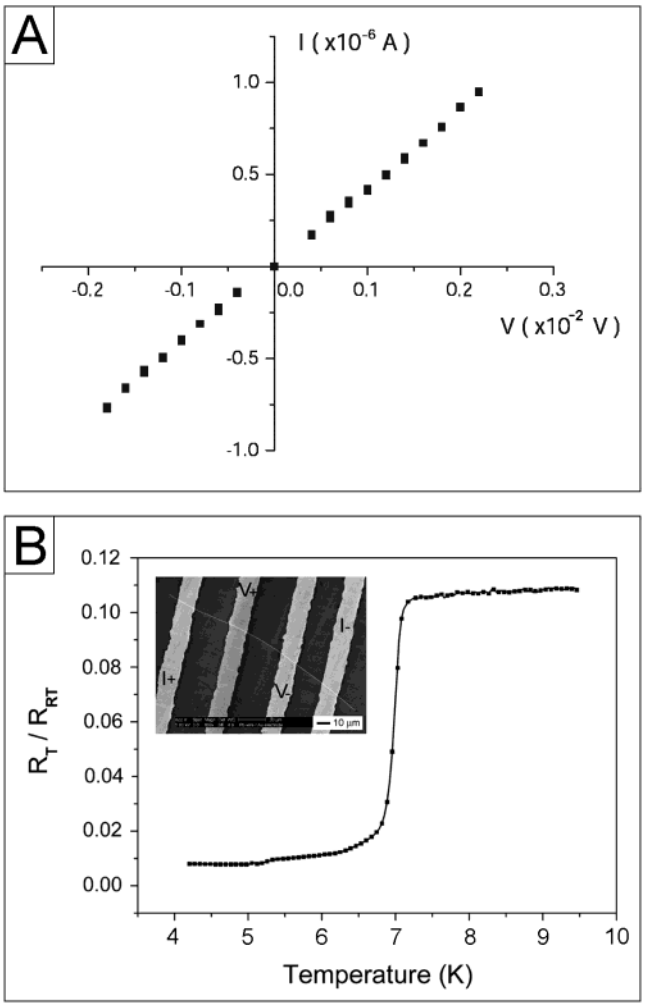

Figure 8. (A) Typical $I-V$ curve for a lead nanowire ~50 nm in diameter at room temperature. (B) A plot showing the dependence of resistance on temperature for the same lead nanowire tested in (A). The resistance was normalized against the value recorded at room temperature. The inset in (B) shows an SEM image of the typical setup used for the four-probe transport measurement, where a single lead nanowire was deposited on four gold electrodes equally separated by 25 μm. The electrodes denoted with I+ and I− were used as sources for current feeding; V+ and V− were used for measuring the potential drop. The resistances recorded here exhibited a clear transition to the superconducting state at a critical temperature similar to that of bulk lead.

of multiple nanowires by directly attaching contacts to the top and bottom surfaces of a membrane template. The measured resistance was, therefore, an averaged response from a large number of nanowires that were inevitably different in diameter, structure, composition, and crystallinity. Most recently, Michotte et al. reported their study on the electron transport properties of individual lead nanowires, where the wires were also embedded in the porous polycarbonate membrane used for electrochemical deposition.[11] By introducing a clever design for the contact, these authors were able to observe the transport properties of individual nanowires. Since the lead nanowires synthesized by the present method were single crystalline in structure and characterized by uniform diameters, it is clearly a big advantage to directly use them for electron transport studies.

We studied the electron transport properties of as-synthesized lead nanowires using the four-probe technique. Because of the relatively high reactivity of these nanowires, freshly prepared samples (within a few hours after synthesis) were used for all measurements. We have also concentrated on individual wires, rather than bundles or aggregates of nanowires. The contacts in such a measurement were realized by first depositing a single lead nanowire through solvent evaporation on the four gold electrodes that had been patterned in advance on a glass slide, and then thermally annealing the regions in physical contact via brief exposure to the electron beam of a scanning electron microscope. Due to the relatively low melting point of lead, this process assured a good contact between the lead nanowire and the gold electrode. Note that exposure to the electron beam for a prolonged period should be avoided. Otherwise, the leads could melt as a result of resistive heating. Wang et al. also described a similar observation in their TEM study.[12] As restricted by the low melting point of lead, the testing current used in all measurements had to be kept below 1.5 μA to avoid any possible melting of the nanowires.

Depending on the lateral dimensions of the lead nanowire, its resistance measured at room temperature could vary in the range from hundreds of ohms to several kiloohms. The current−voltage ($I-V$) plots from these measurements exclusively exhibited a linear dependence for every single nanowire we have tested. Figure 8A shows the typical plot for a nanowire whose lateral dimension was around 50 nm. This $I-V$ plot recorded at room temperature gives a resistance around 2.5 kΩ, and a conductivity of 4.0×10^4 S/cm could be derived from the liner plot, which is very close to the value reported for bulk lead (4.8×10^4 S/cm). We further studied the electron transport properties associated with individual lead nanowires of various diameters at lower temperatures. It was found that the resistance of an individual nanowire responded accordingly to the temperature: the lower the temperature was, the smaller the

resistance would be. When the temperature dropped to ~8 K, its resistance was only about 10% of the value recorded at room temperature (Figure 8B). A sharp change in resistance (5−6 times when compared to the resistance at 8 K) was observed when the temperature was reduced to 7 K, indicating that the nanowire had entered a superconducting state. As the temperature was further decreased, the ratio between R_T and R_{8K} continued to decrease, but at a slower rate. In the work by Michotte et al., a similar result was also obtained for individual lead nanowires of ~40 nm in diameter. However, the resistance never dropped to zero in all our measurements. This observation might be related to the fact that the resistive heating could slowly transform the wire surface to a thin layer of lead oxide while the temperature was still above the transition temperature. It has been shown in previous studies that the transition temperature sometime decreased as the diameter of nanowires (prepared via electrodeposition against templates) was reduced.[4c,13] This dependence suggests the introduction of disorder into a nanowire and thus a weakening in the superconducting property.[13] For all lead nanowires with diameters down to ~50 nm, we did not observe any significant difference in their critical transition temperatures. It was demonstrated that all of them exhibited a sharp drop in resistance at a critical temperature similar to the value reported for bulk lead (7.2 K). It is believed that the single crystalline structure of our nanowires might be the major reason for the elimination of the size-dependent effect.

Conclusions

We have demonstrated a simple and practical route to the large-scale production of single crystalline nanowires of lead as uniform sample and with diameters ranging from 50 to 90 nm. Some of these nanowires could be grown up to several millimeters in length. The formation of such highly anisotropic nanostructures in an isotropic medium was believed to involve a combination of Ostwald ripening (responsible for the transport of material) and the so-called solution−liquid−solid mechanism (to account for the unidirectional growth). The nanowires were shown to exhibit a transition into the superconducting state at a critical temperature of 7.13 K, and no significant difference was observed for nanowires with diameters down to ~50 nm. This observation further confirms that the lead nanowires synthesized using the present method were single crystals, and there were essentially no defects in each individual wire. It is believed that this synthetic route could be potentially extended to several other metals (e.g., Bi and Sn) that are also characterized by relatively low melting points. The availability of such uniform nanowires in high qualities and large quantities will certainly help us achieve a better understanding on the electron transport properties of these solid materials at reduced dimensionalities and sizes.

Supporting Information Available: Histogram of the diameter distributions for more than 50 lead nanowires based on SEM measurements. This material is available free of charge via the Internet at http://pubs.acs.org.

Acknowledgment. This work has been supported in part by an AFOSR-DURINT subcontract from SUNY Buffalo, a Career Award from the National Science Foundation (DMR-9983893), and a Fellowship from the David and Lucile Packard Foundation. Y.X. is an Alfred P. Sloan Research Fellow and a Camille Dreyfus Teacher Scholar. We thank Professor David Cobden for suggesting the synthetic target described in this article. Y.W. thanks Drs. Yugang Sun and Brian Mayers for their help with TEM and HRTEM.

References and Notes

(1) See, for example: (a) a special issue on one-dimensional nanostructures: *Adv. Mater.* **2003**, *15*, 341. (b) A special issue on nanowires: *MRS Bull.* **1999**, *24*, 20. (c) Hu, J.; Odom, T.; Lieber, C. *Acc. Chem. Res.* **1999**, *32*, 435.

(2) (a) Kovtyukhova, N.; Mallouk, T. *Chem. Eur. J.* **2002**, *8*, 4355. (b) Murphy, C.; Jana, N. *Adv. Mater.* **2002**, *14*, 80. (c) El-Sayed, M. *Acc. Chem. Res.* **2001**, *34*, 257. (d) Song, J.; Wu, Y.; Messer, B.; Kind, H.; Yang, P. *J. Am. Chem. Soc.* **2001**, *123*, 10 398. (e) Martin, C.; Mitchell, D. *Electroanal. Chem.* **1999**, *21*, 1.

(3) Kittel, C. *Introduction to Solid State Physics*; John Wiley & Sons: New York, 1996.

(4) (a) Dubois, S.; Michel, A.; Eymery, J.; Duvail, J.; Piraux, L. *J. Mater. Res.* **1999**, *14*, 665. (b) Michotte, S.; Piraux, L.; Dubois, S.; Pailloux, F.; Stenuit, G.; Govaerts, J. *Physica C* **2002**, *377*, 267. (c) Yi, G.; Schwarzacher, W. *Appl. Phy. Lett.* **1999**, *74*, 1746. (d) Jalochowski, M.; Bauer, E. *Surf. Sci.* **2001**, *480*, 109. (e) Jalochowski, M.; Bauer, E. *Prog. Surf. Sci.* **2001**, *67*, 79. (f) Pang, Y.; Meng, G.; Zhang, L.; Shan, W.; Gao, X.; Zhao, A.; Mao, Y. *J. Phys.: Condens. Matter* **2002**, *14*, 11 729. (g) Pang, Y.; Meng, G.; Zhang, L.; Qin, Y.; Gao, X.; Zhao, A.; Fang, Q. *Adv. Func. Mater.* **2002**, *12*, 719.

(5) (a) Sun, Y.; Gates, B.; Mayers, B.; Xia, Y. *Nano Lett.* **2002**, *2*, 165. (b) Sun, Y.; Yin, Y.; Mayers, B.; Herricks, T.; Xia, Y. *Chem. Mater.* **2002**, *14*, 4736. (c) Sun, Y.; Xia, Y. *Adv. Mater.* **2002**, *14*, 833. (d) Sun, Y.; Mayers, B.; Herricks, T.; Xia, Y. *Nano Lett.* **2003**, *3*, 955.

(6) (a) Mohamed, M.; Halawy, S.; Ebrahim, M. *Thermochim. Acta* **1994**, *236*, 249. (b) Leibold, R.; Huber, F. *J. Therm. Anal.* **1980**, *18*, 493. (c) Mu, J.; Perlmutter, D. *Thermochim. Acta* **1981**, *49*, 207.

(7) (a) Trentler, T.; Hickman, K.; Goel, S.; Viano, A.; Gibbons, P.; Buhro, W. *Science* **1995**, *270*, 1791. (b) Trentler, T.; Goel, S.; Hickman, K.; Viano, A.; Chiang, M.; Beatty, A.; Gibbons, P.; Buhro, W. *J. Am. Chem. Soc.* **1997**, *119*, 2172. (c) Markowitz, P.; Zach, M.; Gibbons, P.; Penner, R.; Buhro, W. *J. Am. Chem. Soc.* **2001**, *123*, 4502. (d) Holmes, J.; Johnston, K.; Doty, R.; Korgel, B. *Science* **2000**, *287*, 1471.

(8) Roosen, A.; Carter, W. *Physica A* **1998**, *261*, 232.

(9) (a) Jin, R.; Cao, Y.; Mirkin, C.; Kelly, K.; Schatz, G.; Zheng, J. *Science* **2001**, *294*, 1901. (b) Sun, Y.; Xia, Y. *Science* **2002**, *298*, 2176. (c) Sun, Y.; Mayers, B.; Xia, Y. *Nano Lett.* **2003**, *3*, 675. (d) Maillard, M.; Giorgio, S.; Pileni, M.-P. *Adv. Mater.* **2002**, *14*, 1084. (e) Kirkland, A.; Jefferson, D.; Duff, D.; Edwards, P.; Gameson, I.; Johnson, B.; Smith, D. *Proc. R. Soc. London A* **1993**, *440*, 589. (f) Allpress, J.; Sanders, J. *Surf. Sci.* **1967**, *7*, 1.

(10) Sankarapapavinasam, S.; Ahmed, M. *J. Electrochem. Soc. India* **1990**, *39*, 251.

(11) (a) Michotte, S.; Matefi-Tempfli, S.; Piraux, L. *Appl. Phys. Lett.* **2003**, *82*, 4119. (b) Michotte, S.; Matefi-Tempfli, S.; Piraux, L. *Physica C* **2003**, *391*, 369.

(12) Pan, Z.; Dai, Z.; Wang, Z. *Appl. Phys. Lett.* **2002**, *80*, 309.

(13) (a) Graybeal, J.; Mankiewich, P.; Dynes, R.; Beasley, M. *Phys. Rev. Lett.* **1987**, *59*, 2697. (b) Sharifi, F.; Herzog, A.; Dynes, R. *Phys. Rev. Lett.* **1993**, *71*, 428. (c) Herzog, A.; Xiong, P.; Sharifi, F.; Dynes, R. *Phys. Rev. Lett.* **1996**, *76*, 668.